

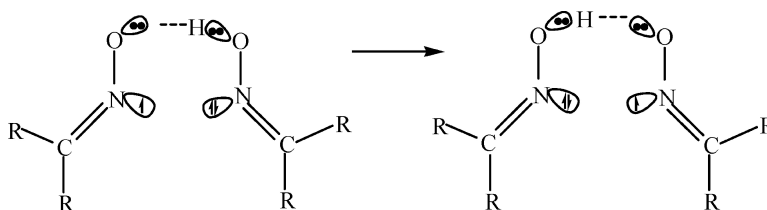
Article

A Theoretical Study of the Iminoxy/Oxime Self-Exchange Reaction. A Five-Center, Cyclic Proton-Coupled Electron Transfer

Gino A. DiLabio, and K. U. Ingold

J. Am. Chem. Soc., **2005**, 127 (18), 6693-6699 • DOI: 10.1021/ja0500409 • Publication Date (Web): 15 April 2005

Downloaded from <http://pubs.acs.org> on March 25, 2009



5-center, cyclic proton coupled electron transfer

More About This Article

Additional resources and features associated with this article are available within the HTML version:

- Supporting Information
- Links to the 8 articles that cite this article, as of the time of this article download
- Access to high resolution figures
- Links to articles and content related to this article
- Copyright permission to reproduce figures and/or text from this article

[View the Full Text HTML](#)



ACS Publications
 High quality. High impact.

A Theoretical Study of the Iminoxyl/Oxime Self-Exchange Reaction. A Five-Center, Cyclic Proton-Coupled Electron Transfer

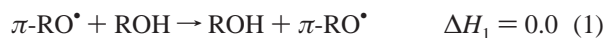
Gino A. DiLabio* and K. U. Ingold

Contribution from the National Institute for Nanotechnology, National Research Council, 9107 116th Street, Edmonton, AB, Canada T6G 2V4, and National Research Council, 100 Sussex Drive, Ottawa, ON, Canada K1A 0R6

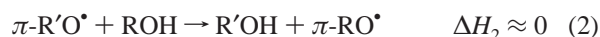
Received January 4, 2005; E-mail: Gino.DiLabio@nrc.ca

Abstract: In solution, the self-exchange reactions for oxygen-centered π -radicals, e.g., $\text{PhO}^\bullet + \text{PhOH} \rightleftharpoons \text{PhOH} + \text{PhO}^\bullet$, are known to occur with low activation enthalpies ($E_a \approx 2$ kcal/mol). For the $\text{PhO}^\bullet/\text{PhOH}$ couple and, we conclude, for other O-centered π -radicals, exchange occurs by proton-coupled electron transfer (PCET) with the proton transferred between oxygen electron pairs while the electron migrates between oxygen orbitals orthogonal to the $-\text{O}-\text{H}-\text{O}-$ transition state plane (Mayer et al. *J. Am. Chem. Soc.* **2002**, *123*, 11142). Iminoxyls, $\text{R}_2\text{C}=\text{NO}^\bullet$, are σ -radicals with substantial spin density on the nitrogen. The $\text{R}_2\text{C}=\text{NO}^\bullet/\text{R}_2\text{C}=\text{NOH}$ self-exchange has a significant E_a (Mendenhall et al. *J. Am. Chem. Soc.* **1973**, *95*, 627). For this exchange, DFT calculations have revealed a counterintuitive cisoid transition state in which the seven atoms, $>\text{C}=\text{NO}-\text{H}-\text{ON}=\text{C}<$, lie in a plane ($\text{R} = \text{H}, \text{Me}$) or, for steric reasons, two planes twisted at 45.2° ($\text{R} = \text{Me}_3\text{C}$). The planar transition state has the two N–O dipoles close to each other and pointing in the same direction and an $\text{O}-\text{H}-\text{O}$ angle of 165.4° . A transoid transition state for $\text{R} = \text{H}$ lies 3.4 kcal/mol higher in energy than the cisoid despite a more favorable arrangement of the dipoles and a near linear $\text{O}-\text{H}-\text{O}$. It is concluded that iminoxyl/oxime self-exchange reactions occur by a five-center, cyclic PCET mechanism with the proton being transferred between electron pairs on the oxygens and the electron migrating between in-plane orbitals on the two nitrogens ($R_{\text{N-N}} = 2.65 \text{ \AA}$). The calculated E_a values (8.8–9.9 kcal/mol) are in satisfactory agreement with the limited experimental data.

In π -radicals the singly occupied molecular orbital (SOMO) is orthogonal to the plane of the local molecular framework, whereas in σ -radicals the SOMO lies in this plane. It is well-established that the self-exchange reactions of oxygen-centered π -radicals, reaction 1,



and other thermoneutral (or near thermoneutral) reactions involving the destruction and formation of oxygen-centered π -radicals, reaction 2,



have remarkably low activation energies, E_a ; see Table 1. Furthermore, the experimental data indicate that when one, or both, of the oxygen atoms is sterically shielded, reactions 1 and 2 are slow because of substantial entropic barriers; that is, these reactions have unusually low Arrhenius A -factors for hydrogen atom transfer (HAT) processes; see Table 1.^{1–12} However, when neither oxygen is sterically shielded, the A -factors are larger

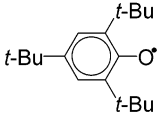
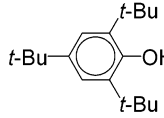
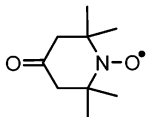
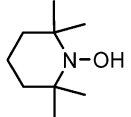
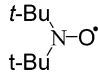
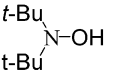
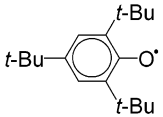
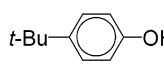
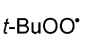
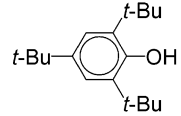

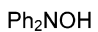
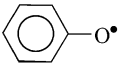
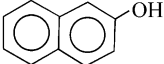
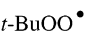
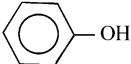
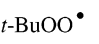
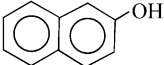
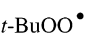
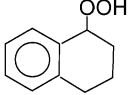
and may approach (or, for exothermic reactions, may even surpass)¹³ values that are “normal” for HAT reactions, viz.,¹⁵ $10^{8.5 \pm 0.5} \text{ M}^{-1} \text{ s}^{-1}$; see Table 1.

Mayer et al.’s¹⁶ detailed theoretical study of the phenoxyl/phenol self-exchange reaction revealed the exciting fact that this is not a simple HAT process in which the proton is transferred together with one of its bonding electrons.¹⁷ Rather, the $\text{PhO}^\bullet/\text{PhOH}$ self-exchange is a *proton-coupled electron transfer*

(1) Kreilick, R. W.; Weissman, S. I. *J. Am. Chem. Soc.* **1966**, *88*, 2645–2652. See also: Kreilick, R. W.; Weissman, S. I. *J. Am. Chem. Soc.* **1962**, *84*, 306–307. Arick, M. R.; Weissman, S. I. *J. Am. Chem. Soc.* **1968**, *90*, 1654.
(2) Mader, E. A.; Larsen, A. S.; Mayer, J. M. *J. Am. Chem. Soc.* **2004**, *126*, 8066–8067.

(3) Lucarini, M.; Pedrielli, P.; Pedulli, G. F.; Cabiddu, S.; Fattuoni, C. *J. Org. Chem.* **1996**, *61*, 9259–9263.
(4) Mahoney, L. R.; DaRooge, M. A. *J. Am. Chem. Soc.* **1970**, *92*, 890–899.
(5) DaRooge, M. A.; Mahoney, L. R. *J. Org. Chem.* **1967**, *32*, 1–6.
(6) Mahoney, L. R.; DaRooge, M. A. *J. Am. Chem. Soc.* **1970**, *92*, 4063–4067.
(7) Howard, J. A.; Furimsky, E. *Can. J. Chem.* **1973**, *51*, 3738–3745.
(8) Mahoney, L. R.; DaRooge, M. A. *J. Am. Chem. Soc.* **1975**, *97*, 4722–4731.
(9) Foti, M.; Ingold, K. U.; Luszyk, J. *J. Am. Chem. Soc.* **1994**, *116*, 9440–9447.
(10) Chenier, J. H. B.; Furimsky, E.; Howard, J. A. *Can. J. Chem.* **1974**, *52*, 3682–3688.
(11) Korcek, S.; Chenier, J. H. B.; Howard, J. A.; Ingold, K. U. *Can. J. Chem.* **1972**, *50*, 2285–2297.
(12) Chenier, J. H. B.; Howard, J. A. *Can. J. Chem.* **1975**, *53*, 623–627.
(13) For example,⁹ in a rate-retarding hydrogen bond accepting solvent system¹⁴ (di-*tert*-butyl peroxide/acetonitrile, 2:1, v/v, containing 1.4 M phenol) the reaction $\text{PhO}^\bullet + \alpha\text{-tocopherol} \rightarrow \text{PhOH} + \alpha\text{-tocopheroxyl}$, for which $\Delta H = -10.1$ kcal/mol,³ has $\log(A/\text{M}^{-1} \text{ s}^{-1}) = 10.0$ and $E_a = 2.0$ kcal/mol.
(14) Snelgrove, D. W.; Luszyk, J.; Banks, J. T.; Mulder, P.; Ingold, K. U. *J. Am. Chem. Soc.* **2001**, *123*, 469–477.
(15) Benson, S. W. *Thermochemical kinetics*, 2nd ed.; Wiley: New York, 1976.
(16) Mayer, J. M.; Hrovat, D. A.; Thomas, J. L.; Borden, W. T. *J. Am. Chem. Soc.* **2002**, *124*, 11142–11147.

Table 1. Arrhenius Parameters and Ambient Temperature Rate Constants for Some Thermoneutral, or Nearly Thermoneutral, Hydrogen Atom Transfers between Oxygen-Centered π -Radicals

RO \cdot / R'O \cdot <i>Both Reactants Sterically Shielded</i>	ROH	$\Delta H_{1/2}$ (kcal/mol)	$\log A_{1/2}$ (M $^{-1}$ s $^{-1}$)	E_a (kcal/mol)	k M $^{-1}$ s $^{-1}$	Ref.
		0.0	3.7	1.2	6.6×10^2	1
		~ -2.0	3.8 ^a	3.8 ^a	10	2
		0.0	5.1 ^b	3.5 ^b	3.3×10^2	1
<i>One Reactant Sterically Shielded</i>						
		$\sim +4.2^c$	5.5 ^d	4.8	93	4,5
		$\sim -7.0^e$	4.2	0.5	$7 \times 10^3^f$	7
<i>No Steric Shielding</i>						
		0.0	(> 7)		$> 10^7$	1
		-2.2 ^g	8.3	2.3	$4 \times 10^6^f$	9
		+0.3 ^g	7.2	5.2	3×10^3	10
		-1.9 ^g	6.4	2.6	3×10^4	10
		$\sim +1.4^h$	6.0	4.5	7×10^2	12

^a Derived from Figure S5 in the Supporting Information of ref 2. ^b Estimated from ref 1 using the given rate constant at 27 °C and Figure 10, bottom, which shows a plot of line broadening vs $1/T$ in the temperature range 40 to 84 °C. ^c Reference 3. ^d $\log A/M^{-1} s^{-1}$ for five non-ortho-substituted phenols lie in the range 6.0 ± 0.5 ; see ref 4. ^e For tetralylperoxyl, see ref 6. ^f Calculated at 298 K from the Arrhenius parameters. ^g Reference 8. ^h Based on the fact that tertiary alkylperoxyls are only 10% as reactive in H-atom abstractions as secondary alkylperoxyls; see ref 11.

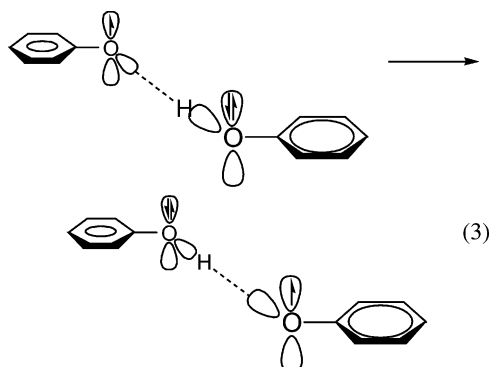
(PCET) with the proton and electron being transferred between different sets of orbitals.¹⁸ The reaction involves the initial

(17) However, the apparently analogous PhCH $_2$ \cdot /PhCH $_3$ self-exchange is a HAT reaction, and its transition state is 18.3 kcal/mol higher in energy than the separated reactants.¹⁶

(18) For a review of PCET, see: Mayer, J. M. *Annu. Rev. Phys. Chem.* **2004**, *55*, 363–390. For some interesting PCET vs HAT papers published after this review, see, e.g., ref 2 and: Anglada, J. M. *J. Am. Chem. Soc.* **2004**, *126*, 9809–9820. Olivella, S.; Anglada, J. M. Sole, A.; Bofill, J. M. *Chem. Eur. J.* **2004**, *10*, 3404–3410. Rhile, I. J.; Mayer, J. M. *J. Am. Chem. Soc.* **2004**, *126*, 12718–12719. Shukla, D.; Young, R. H.; Farid, S. *J. Phys. Chem. A* **2004**, *108*, 10386–10394. Terecek, F.; Syrstad, E. A. *J. Am. Chem. Soc.* **2003**, *125*, 3353–3369.

formation of a hydrogen-bonded complex, PhO \cdot ...HOPh, which lies 9.9 kcal/mol lower in energy than the separated reactants. The transition state is also lower in energy than the separated reactants (by 1.3 kcal/mol), which implies that self-exchange is essentially a diffusion-controlled reaction. The transition state is close to planar. The proton is transferred nearly in the plane of the two phenoxyls and is a part of a *four-electron, three-center H-bond* involving a σ lone pair on the oxygen of PhO \cdot and the O–H bond of PhOH.¹⁹ Accompanying this proton transfer between oxygen σ lone pairs is the transfer in the same

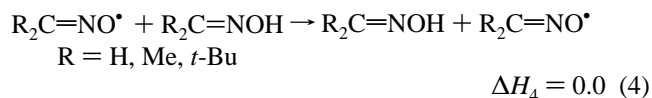
direction of an electron from the orthogonal, doubly occupied $2p-\pi$ atomic orbital (AO) on oxygen in PhOH to the singly occupied $2p-\pi$ AO of PhO \cdot . That is, in simplified AO form showing only the relevant orbitals, this PCET reaction can be represented as



It seems reasonable to assume that most, and possibly all, of the *formal* HAT reactions shown in Table 1 and analogous reactions involving the destruction and formation of oxygen-centered π -radicals will also occur via PCET. This is because all of the radicals will be fairly strong H-bond acceptors (like PhO \cdot) and all the substrates will be fairly strong H-bond donors (like PhOH). Strong radical/molecule complexes will therefore be formed. Moreover, there will be strong π -electron-donation from both R groups to their attached oxygen atoms in the transition states for these H-atom transfer processes. Thus, there will be strong, four-electron proton binding, which will favor PCET and disfavor HAT mechanisms.

In the present paper we address the question: *Does the formal HAT between oxygen-centered σ -radicals occur by a HAT or by a PCET mechanism?*²⁰

To answer this question, we have examined the iminoxyl/oxime self-exchange, reaction(s) 4,



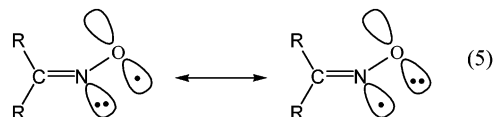
The results of these computations are then compared with the only available experimental data on this reaction.²²

Results

Theoretical Computations. Calculations on the $\text{H}_2\text{C}=\text{NO}\cdot/\text{H}_2\text{C}=\text{NOH}$ pair and on the $\text{Me}_2\text{C}=\text{NO}\cdot/\text{Me}_2\text{C}=\text{NOH}$ pair were performed at the UB3LYP^{23,24}/6-31+G** level using the Gaussian 03 suite of programs.²⁵ To keep the computational time reasonable for the *t*-Bu $_2\text{C}=\text{NO}\cdot/t$ -Bu $_2\text{C}=\text{NOH}$ pair, a locally dense basis set (LDBS) approach was employed in which

the C=NO(H) were represented with 6-31+G** basis sets and the *t*-Bu groups were represented with the smaller 6-31G* basis sets. It has been demonstrated that the LDBS approach can accurately reproduce transition state properties.²⁶ Reported energies do not include zero-point vibration corrections.

Structure of Iminoxyl Radicals. (i) Experimental. Iminoxyl radicals were first identified in solution by Thomas²⁷ in 1964 using EPR spectroscopy, and the *Z*-*E* isomerization of non-symmetric iminoxyls, RR'C=NO \cdot , was also described. On this basis, and on the basis of their large nitrogen splitting ($a_N \approx 28$ –33 G), which indicates that there is significant spin density on nitrogen in an orbital with considerable s character, Thomas concluded that the unpaired electron resides in a π -type orbital lying in the plane of the local molecular framework. That is, Thomas²⁷ concluded that iminoxyls are σ -radicals. They can be represented by the canonical structures



Thomas's conclusions have been amply confirmed by EPR^{28,29} and other studies.³⁰ In addition, Symons²⁸ has estimated that, independent of the nature of the R groups, $41 \pm 5\%$ of the spin density in $\text{R}_2\text{C}=\text{NO}\cdot$ is on the nitrogen in an orbital with a p/s ratio of 6.1 ± 0.7 . There has been no X-ray crystallographic study of an iminoxyl.³¹

(ii) Calculations. A spin density map for $\text{H}_2\text{C}=\text{NO}\cdot$ is shown in Figure 1. The calculated Mulliken spin densities on the O and N atoms are +0.57 and +0.45 (calculated $a_N = 29.5$ G), in satisfactory agreement with Symons' EPR estimate.²⁸ Similarly, for $\text{Me}_2\text{C}=\text{NO}\cdot$ and *t*-Bu $_2\text{C}=\text{NO}\cdot$ the calculated oxygen/nitrogen spin densities are +0.57/+0.46 (calculated $a_N = 30.5$ G) and +0.53/+0.48 (calculated $a_N = 30.4$ G), respectively. As a result of this delocalization of the unpaired electron (see eq 5), the N–O bond in iminoxyls acquires double-bond character

(23) Becke, A. D. *J. Chem. Phys.* **1993**, *98*, 5648–5642.

(24) Lee, C.; Yang, W.; Parr, R. G. *Phys. Rev. B* **1988**, *37*, 785–789.

(25) Frisch, M. J.; Trucks, G. W.; Schlegel, H. B.; Scuseria, G. E.; Robb, M. A.; Cheeseman, J. R.; Montgomery, Jr., J. A.; Vreven, T.; Kudin, K. N.; Burant, J. C.; Millam, J. M.; Iyengar, S. S.; Tomasi, J.; Barone, V.; Mennucci, B.; Cossi, M.; Scalmani, G.; Rega, N.; Petersson, G. A.; Nakatsuji, H.; Hada, M.; Ehara, M.; Toyota, K.; Fukuda, R.; Hasegawa, J.; Ishida, M.; Nakajima, T.; Honda, Y.; Kitao, O.; Nakai, H.; Klene, M.; Li, X.; Knox, J. E.; Hratchian, H. P.; Cross, J. B.; Bakken, V.; Adamo, C.; Jaramillo, J.; Gomperts, R.; Stratmann, R. E.; Yazyev, O.; Austin, A. J.; Cammi, R.; Pomelli, C.; Ochterski, J. W.; Ayala, P. Y.; Morokuma, K.; Voth, G. A.; Salvador, P.; Dannenberg, J. J.; Zakrzewski, V. G.; Dapprich, S.; Daniels, A. D.; Strain, M. C.; Farkas, O.; Malick, D. K.; Rabuck, A. D.; Raghavachari, K.; Foresman, J. B.; Ortiz, J. V.; Cui, Q.; Baboul, A. G.; Clifford, S.; Cioslowski, J.; Stefanov, B. B.; Liu, G.; Liashenko, A.; Piskorz, P.; Komaromi, I.; Martin, R. L.; Fox, D. J.; Keith, T.; Al-Laham, M. A.; Peng, C. Y.; Nanayakkara, A.; Challacombe, M.; Gill, P. M. W.; Johnson, B.; Chen, W.; Wong, M. W.; Gonzalez, C.; and Pople, J. A. *Gaussian 03*, Revision C.02; Gaussian, Inc.: Wallingford, CT, 2004.

(26) DiLabio, G. A. *J. Phys. Chem. A* **1999**, *103*, 11414–11424.

(27) Thomas, J. R. *J. Am. Chem. Soc.* **1964**, *86*, 1446–1447.

(28) Symons, M. C. R. *J. Chem. Soc.* **1965**, 2276–2277. Fox, W. M.; Symons M. C. R. *J. Chem. Soc. A* **1966**, 1503–1507.

(29) See, for example: (a) Gilbert, B. C.; Norman, R. O. C.; Price, D. C. *Proc. Chem. Soc.* **1964**, 234. (b) Lemaire, H.; Rassat, A. *Tetrahedron Lett.* **1964**, 2245–2248. (c) Gilbert, B. C.; Norman, R. O. C. *J. Chem. Soc. B* **1966**, 86–91. (d) Brokenshire, J. L.; Roberts, J. R.; Ingold, K. U. *J. Am. Chem. Soc.* **1972**, *94*, 7040–7049. (e) Dobashi, T. S.; Parker, D. R.; Grubbs, E. J. *J. Am. Chem. Soc.* **1977**, *99*, 5382–5387. (f) Mackor, A. *J. Org. Chem.* **1978**, *43*, 3241–3243. (g) Lucarini, M.; Pedulli, G. F.; Alberti, A. *J. Org. Chem.* **1994**, *59*, 1980–1983.

(30) Pratt, D. A.; Blake, J. A.; Mulder, P.; Walton, J. C.; Korth, H.-G.; Ingold, K. U. *J. Am. Chem. Soc.* **2004**, *126*, 10667–10675.

(31) Lindsay, B.; Horswill, E. C.; Davidson, D. W.; Ingold, K. U. *Can. J. Chem.* **1974**, *52*, 3554–3556.

(19) This contrasts with the three-electron, three-center transition state for the PhCH $_2$ /PhCH $_3$ HAT self-exchange. The transition state for a HAT PhO \cdot /PhOH self-exchange is 5.8 kcal/mol *higher* in energy than the separated reactants.

(20) Free alkoxy radicals (i.e., non-H-bonded) cannot be categorized as either π - or σ -radicals because their SOMO is degenerate; that is, it has no fixed orientation with respect to the rest of the radical. For the CH $_3\text{O}\cdot$ /CH $_3\text{OH}$ self-exchange, Mayer et al.'s¹⁶ DFT calculations indicate a three-electron interaction and hence a HAT process, the PCET alternative being disfavored because of the poor π -donor ability of the methyl groups. Their computed E_a is consistent with a measured E_a for a more sterically congested alkoxy/alcohol pair.²¹

(21) Griller, D.; Ingold, K. U. *J. Am. Chem. Soc.* **1974**, *96*, 630–632.

(22) Mendenhall, G. D.; Ingold, K. U. *J. Am. Chem. Soc.* **1973**, *95*, 627–628.

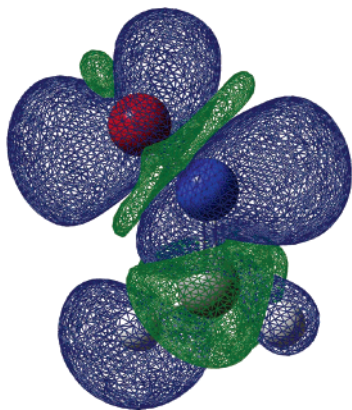


Figure 1. Spin density map of $\text{H}_2\text{C}=\text{NO}^\bullet$. Blue indicates regions of positive spin density, while green indicates regions of negative spin density.

and is considerably shorter in the radical than in the oxime, e.g., 1.23 Å in $\text{H}_2\text{C}=\text{NO}^\bullet$ vs 1.40 Å in $\text{H}_2\text{C}=\text{NOH}$,³² and the CNO angle is considerably larger in the radical, e.g., 134.7° in $\text{H}_2\text{C}=\text{NO}^\bullet$ vs 111.3° in $\text{H}_2\text{C}=\text{NOH}$.³²

In iminoxyl radicals the in-plane oxygen sp^3 orbital adopts lone pair character (eq 5) and the remaining oxygen lone pair orbitals lie in a plane perpendicular to the $\text{R}_2\text{C}=\text{NO}^\bullet$ plane and are “rabbit ears” directed away from the R_2CN moiety. The σ -radical character of $\text{H}_2\text{C}=\text{NO}^\bullet$ is illustrated by the spin density map shown in Figure 1.

Calculated Structures and Energies of the $\text{H}_2\text{C}=\text{NO}^\bullet/\text{H}_2\text{C}=\text{NOH}$ Hydrogen-Bonded Pair. The lowest energy for this iminoxyl/oxime pair has a nearly planar overall structure. The iminoxyl’s in-plane oxygen orbital that is involved in the partial π -bond with the adjacent N atom is the H-bond acceptor (HBA). This H-bonding arrangement is accompanied by a strong electrostatic attraction between other portions of the iminoxyl and oxime, including a C–H...N interaction between the iminoxyl’s CH_2 group and the oxime’s nitrogen (H...N distance = 2.63 Å); see Figure 2. It is these electrostatic interactions that explain why a transoid arrangement of the HBA and H-bond donor (HBD), of the type involved in the PhO^\bullet ... HOPh complex, *vide supra*, is not observed for $\text{H}_2\text{C}=\text{NO}^\bullet$... $\text{HON}=\text{CH}_2$. The energy (enthalpy) of the favored H-bonded $\text{H}_2\text{C}=\text{NO}^\bullet$... $\text{HON}=\text{CH}_2$ pair (Figure 2b) lies 4.2 (2.8) kcal/mol below the separated reactants. The minimum energy structure for a transoid H-bonded pair lies 2.7 kcal/mol below the separated reactants.

Calculated Transition States. The minimum energy iminoxyl/oxime H-bonded pair shown in Figure 2 must undergo an internal rotation as the exchange transition state is approached. This pre-transition state complex (which is like the transition state in Figure 3a but with the transferring H atom not centered between the two oxygen atoms) has a weaker H-bond, and for the $\text{H}_2\text{C}=\text{NO}^\bullet/\text{H}_2\text{C}=\text{NOH}$ pair it is 1.3 kcal/mol weaker than for the ground state H-bonded complex. That is, it is 2.9 kcal/mol below the energy of the free reactants; moreover it is not a local minimum.

The transition states for the self-exchanges, $\text{H}_2\text{C}=\text{NO}^\bullet/\text{H}_2\text{C}=\text{NOH}$ (Figure 3) and $\text{Me}_2\text{C}=\text{NO}^\bullet/\text{Me}_2\text{C}=\text{NOH}$, are both completely symmetric with all seven C=N–O...H...O=N=C

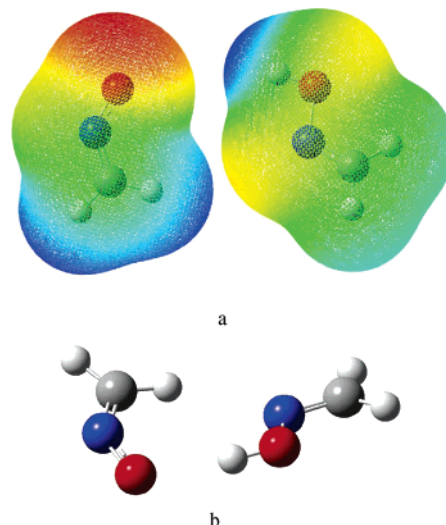


Figure 2. (a) Electrostatic potential surfaces for $\text{H}_2\text{C}=\text{NO}^\bullet$ and $\text{HON}=\text{CH}_2$. Red indicates regions of more negative charge, and blue indicates regions of more positive charge. (b) Hydrogen-bonded $\text{H}_2\text{C}=\text{NO}^\bullet/\text{H}_2\text{C}=\text{NOH}$ complex.

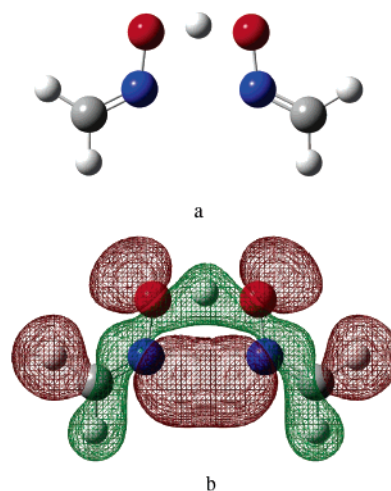


Figure 3. (a) Calculated symmetric transition state for the $\text{H}_2\text{C}=\text{NO}^\bullet/\text{H}_2\text{C}=\text{NOH}$ exchange. (b) Doubly occupied molecular orbital of the transition state for the $\text{H}_2\text{C}=\text{NO}^\bullet/\text{H}_2\text{C}=\text{NOH}$ exchange showing N–N bonding overlap.

atoms being coplanar in a cisoid arrangement with substantial overlap between the orbitals of the lone pairs on the two nitrogen atoms (Figure 3b). These structures were verified to be true transition states by showing that they displayed single negative vibration modes connecting reactants to products.

Conversion of the pre-reaction complex (Figure 2b) to the transition state (Figure 3) while maintaining the hydrogen bond requires either a rotation about the N–O bond of the iminoxyl or an inversion at the iminoxyl’s N atom. Alternatively, the “pre-reaction” complex could dissociate and the free reactants re-engage in a more appropriate conformation for reaction. Of these three possibilities, inversion at nitrogen can be ruled out unequivocally. This is because the inversion of iminoxyl radicals has a high barrier, *viz.*, calculated (kcal/mol) for $\text{H}_2\text{C}=\text{NO}^\bullet$, ca. 12; $\text{Me}_2\text{C}=\text{NO}^\bullet$, 13.1;³⁰ $t\text{-Bu}_2\text{C}=\text{NO}^\bullet$, 10.4;³⁰ measured (kcal/mol) for $(t\text{-Bu})_2\text{C}=\text{NO}^\bullet$, 9.6.³³ Maintaining a hydrogen bond and rotation about the N–O bond of the iminoxyl is the

(32) Similarly, earlier calculations³⁰ have given the following N–O bond lengths and CNO angles: $\text{Me}_2\text{C}=\text{NO}^\bullet$, 1.24 Å, 133.6°; $\text{Me}_2\text{C}=\text{NOH}$, 1.42 Å, 111.0°; $t\text{-Bu}_2\text{C}=\text{NO}^\bullet$, 1.24 Å, 135.8°; $t\text{-Bu}_2\text{C}=\text{NOH}$, 1.41 Å, 116.2°.

(33) Ingold, K. U.; Brownstein, S. *J. Am. Chem. Soc.* **1975**, *97*, 1817–1818.

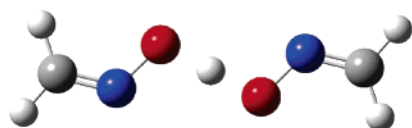


Figure 4. Calculated transoid transition state for the $\text{H}_2\text{C}=\text{NO}^*/\text{H}_2\text{C}=\text{NOH}$ exchange.

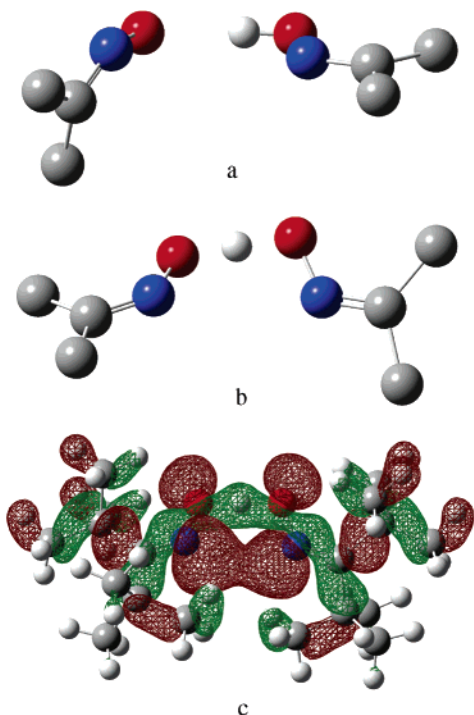


Figure 5. (a) Hydrogen-bonded pre-reaction complex for $t\text{-Bu}_2\text{C}=\text{NO}^*/t\text{-Bu}_2\text{C}=\text{NOH}$ exchange. The methyl groups have been removed for clarity. (b) Cisoid transition state for the $t\text{-Bu}_2\text{C}=\text{NO}^*/t\text{-Bu}_2\text{C}=\text{NOH}$ exchange. The methyl groups have been removed for clarity. (c) Doubly occupied molecular orbital of the transition state for the $t\text{-Bu}_2\text{C}=\text{NO}^*/t\text{-Bu}_2\text{C}=\text{NOH}$ exchange showing N–N bonding overlap.

avored route to the desired cisoid pre-transition state structure because this involves an energy barrier of only 0.5 kcal/mol,³⁴ whereas breaking the H-bond completely would require 4.2 kcal/mol.

For $\text{H}_2\text{C}=\text{NO}^*/\text{H}_2\text{C}=\text{NOH}$ and $\text{Me}_2\text{C}=\text{NO}^*/\text{Me}_2\text{C}=\text{NOH}$ self-exchange reactions the cisoid transition states (Figure 3) have the two large N–O dipoles unfavorably aligned. Therefore, additional calculations were performed on putative transoid transition states that would have reduced dipole/dipole repulsions. These transoid transition states, shown in Figure 4 for $\text{H}_2\text{C}=\text{NO}^*/\text{H}_2\text{C}=\text{NOH}$, have O–H–O distances equal to those of the cisoid transition states and OHO angles of 178.4° vs 165.4° for the cisoid. Both the reduced dipole/dipole interaction and the linear O–H–O arrangement would be expected to favor the transoid transition state. Nevertheless, and very surprisingly, the transoid transition state for self-exchange is 3.4 kcal/mol higher in energy than the cisoid transition state (Figure 3), and it is therefore strongly disfavored.

For the $t\text{-Bu}_2\text{C}=\text{NO}^*/t\text{-Bu}_2\text{C}=\text{NOH}$ pair, steric effects cause the minimum energy H-bonded structure to have a perpendicular arrangement in which the oxime's O–H group is directed toward an out-of-plane oxygen lone pair on the iminoxyl (Figure

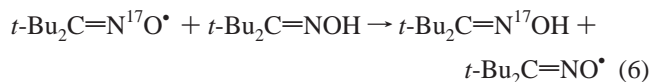
(34) That is, rotation of the iminoxyl radical through 90° gives a structure with a hydrogen bond energy of 3.7 kcal/mol.

5a). Despite the presence of four bulky *tert*-butyl groups, the transition state is again cisoid (Figure 5b,c), but the seven CNO–H–ONC atoms are prevented from lying in a single plane. Instead, the two C=NO planes are inclined at an angle of 45.2° to one another (Figure 5b), which reduces overlap between the orbitals of the nitrogen lone pairs in the transition state for the $t\text{-Bu}_2\text{C}=\text{NO}^*/t\text{-Bu}_2\text{C}=\text{NOH}$ self-exchange (Figure 5c) relative to overlap in the transition state for the $\text{H}_2\text{C}=\text{NO}^*/\text{H}_2\text{C}=\text{NOH}$ exchange (cf. Figure 3b) and the transition state for the $\text{Me}_2\text{C}=\text{NO}^*/\text{Me}_2\text{C}=\text{NOH}$ exchange. Interestingly, this sterically induced de-planarization of the $t\text{-Bu}_2\text{C}=\text{NO}^*/t\text{-Bu}_2\text{C}=\text{NOH}$ transition state produces only a small increase, 0.3 to 1.1 kcal/mol, in the activation energies for self-exchange relative to sterically unencumbered oxime/iminoxyl pairs; see below.

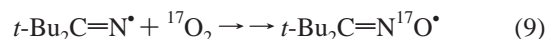
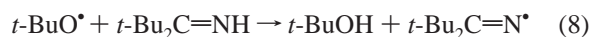


Discussion

Comparison of Measured and Calculated Activation Energies for Iminoxyl/Oxime Self-Exchange Reactions. The kinetics of reaction 6 were measured in 1973 by EPR spectroscopy in benzene at temperatures from 7 to 37°C .²² Isotopic

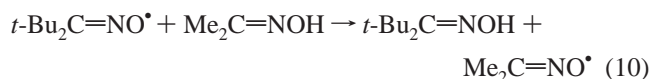


labeling of the iminoxyl was achieved by photolyzing di-*tert*-butyl peroxide and di-*tert*-butylketimine in the presence of oxygen enriched with ^{17}O in the cavity of an EPR spectrometer:



Pseudo-first-order decay of the lowest field satellite of $t\text{-Bu}_2\text{C}=\text{N}^{17}\text{O}^*$ gave $k_6 = 1.3 \pm 0.3 \text{ M}^{-1} \text{ s}^{-1}$ at 25°C and an activation energy of $7 \pm 2 \text{ kcal/mol}$, from which $\log(A_6/\text{M}^{-1} \text{ s}^{-1}) \approx 5.25$. This was not an easy experiment, but E_a is within sight of the 9.9 kcal/mol calculated herein.

An easier EPR kinetic experiment carried out at the same time²² involved the mixing of benzene solutions of the persistent $t\text{-Bu}_2\text{C}=\text{NO}^*$ radical³⁵ (10^{-3} M) with 0.1 M $\text{Me}_2\text{C}=\text{NOH}$ (which yields the transient $\text{Me}_2\text{C}=\text{NO}^*$ radical,^{29d} reaction 10).



The pseudo-first-order decay of the $t\text{-Bu}_2\text{C}=\text{NO}^*$ signal was measured at temperatures from 25 to 51°C . This yielded $k_{10} = 1.1 \times 10^{-4} \text{ M}^{-1} \text{ s}^{-1}$ at 25°C , $\log(A_{10}/\text{M}^{-1} \text{ s}^{-1}) = 9.08$, and $E_a = 17.9 \text{ kcal/mol}$. Since order was recently restored to (the scandal of) oxime O–H bond dissociation enthalpies³⁰ (BDEs),

(35) Mendenhall, G. D.; Ingold K. U. *J. Am. Chem. Soc.* **1973**, *95*, 2963–2971.

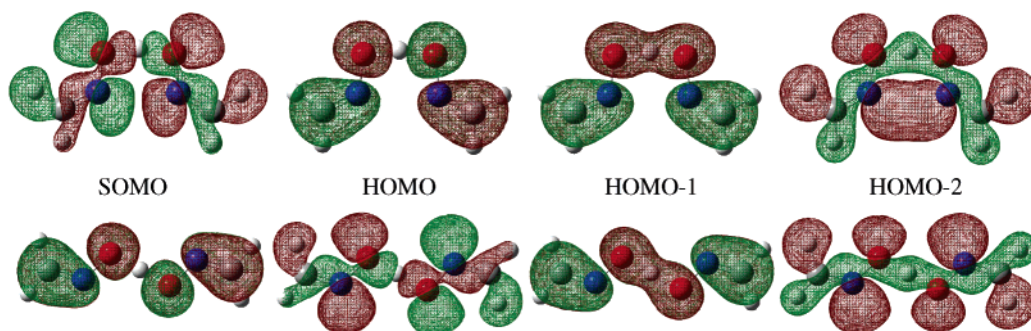


Figure 6. Four highest occupied molecular orbitals for the cisoid (top) and transoid (bottom) transition states. Energy decreases from left to right.

ΔH_{10} is readily calculated as $\text{BDE}[t\text{-Bu}_2\text{C}=\text{NO}-\text{H}] - \text{BDE}[\text{Me}_2\text{C}=\text{NOH}] = 77.6 - 84.6 = -7.0$ kcal/mol. This implies that for a thermoneutral iminoxyl/oxime self-exchange that is somewhat less sterically congested than the $t\text{-Bu}_2\text{C}=\text{NO}^*/t\text{-Bu}_2\text{C}=\text{NOH}$ reaction the activation energy will be less than 17.9 kcal/mol and could possibly be as low as $17.9 - 7.0 = 10.9$ kcal/mol. This lowest possible value is again in reasonable agreement with our present calculated E_a 's (range 8.8–9.9 kcal/mol), particularly in view of the small temperature range covered in the EPR experiments.

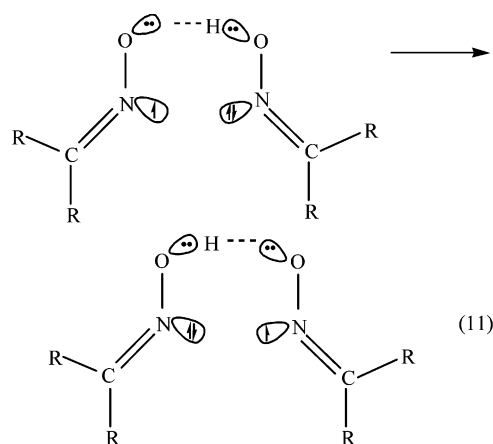
Mechanism of Iminoxyl/Oxime Self-Exchange Reactions.

The intuitive transition state for the iminoxyl/oxime self-exchange is transoid because this would minimize both steric hindrance (particularly in the case of $t\text{-Bu}_2\text{C}=\text{NO}^*/t\text{-Bu}_2\text{C}=\text{NOH}$) and N–O dipole/N–O dipole repulsion. Nevertheless, this transition state for the $\text{H}_2\text{C}=\text{NO}^*/\text{H}_2\text{C}=\text{NOH}$ couple was found to lie 3.4 kcal/mol higher in energy than a counterintuitive, cisoid transition state. This difference in energy must reflect unexpected factors favoring a cisoid self-exchange. The four highest occupied molecular orbitals for the cisoid and transoid transition state structures are shown in Figure 6. For both transition states the SOMO is highest in energy. The lowest energy cisoid orbital (HOMO–2) shows the N–N bonding overlap, while the SOMO is antibonding between these two atoms. The transoid transition state orbitals bear many similarities to the cisoid orbitals. The exception is, of course, the absence in the lowest energy transoid structure of orbital overlap between the two nitrogen atoms (HOMO–2). The presence of a two-center, three-electron bond between nitrogen atoms therefore preferentially stabilizes the cisoid transition state structure.

Despite the differences in bonding in the two transition states, the charge and spin density distributions in the cisoid and transoid transition state structures are very similar (see Supporting Information). This indicates that the exchange reaction through either transition state likely occurs via the same mechanism.

We suggest that the iminoxyl/oxime self-exchange occurs via a five-center, cyclic PCET. The two O–H distances in the transition state (1.19 vs 0.97 Å for the free oxime) are small enough for proton transfer, while the N–N distance of 2.65 Å reflects the overlap of the two nitrogen atoms' lone pair orbitals. Because this overlap is partially bonding, a goodly portion of the electron density is delocalized from the iminoxyl's oxygen to its nitrogen atom (see eq 5 and Figure 1). That is, the electron that will be transferred to the iminoxyl radical is already partly localized on the iminoxyl's nitrogen atom due to the two-center, three-electron bonding interaction between the two nitrogen atoms in the cisoid pre-transition state structure. Thus, self-

exchange involves proton transfer between the two oxygen atoms while concurrently an electron is transferred in the same direction from the oxime nitrogen's sp^2 lone pair to the iminoxyl's nitrogen. In AO terms, and for comparison with the PhO^*/PhOH self-exchange shown in reaction 3, the iminoxyl/oxime self-exchange can be represented as



For the transoid transition state PCET would involve proton transfer between the two oxygen atoms and electron transfer possibly from an electron pair on the oxime's oxygen to the iminoxyl's nitrogen (O–N distance = 3.05 Å) or less probably from the oxime nitrogen's sp^2 lone pair to the iminoxyl's nitrogen (N–N distance = 4.04 Å). The distance the electron must tunnel is much farther in the transoid transition state than in the cisoid transition state, and the transoid transition state is higher in energy than the cisoid transition state; hence the reaction via the transoid transition state is much slower than via the cisoid transition state.

In summary, the iminoxyl/oxime self-exchange adds to the growing number of formal HAT processes that are known to occur by PCET mechanisms.^{2,16,18} Since iminoxyls are σ -radicals, the transferred electron necessarily comes from an orbital lying in-plane with the oxime's O–H bond. However, this electron is *not* one of the electrons making the O–H bond. All iminoxyl/oxime self-exchanges have substantial activation energies that are very much higher than the activation energies for self-exchanges involving oxygen-centered π -radicals. They occur via a five-center, cyclic transition state even in the case of the sterically encumbered $t\text{-Bu}_2\text{C}=\text{NO}^*/t\text{-Bu}_2\text{C}=\text{NOH}$ pair.

Acknowledgment. We sincerely thank two anonymous referees for their extremely helpful comments. We also thank Erin R. Johnson for helpful discussions and the Center of

Excellence in Integrated Nanotools (University of Alberta) for access to computational resources.

Supporting Information Available: Coordinates, vibration frequencies, spin densities, atomic charges, and energies for all

optimized structures. This material is available free of charge via the Internet at <http://pubs.acs.org>.

JA0500409